Available online at www.sciencedirect.com
SCIENCE DIRECT
Polymer 46 (2005) 939–945
polymer
www.elsevier.com/locate/polymer

Thermal deformations of oriented noncrystalline poly (ethylene terephthalate) fibers in the presence of mesophase structure

Jong Kahk Keum, Hyun Hoon Song*

Department of Polymer Science and Engineering, Hannam University, Daejon, South Korea

Received 7 July 2004; received in revised form 1 December 2004; accepted 1 December 2004
Available online 18 December 2004

Abstract

Thermally induced dimensional changes, thermal shrinkage and elongation, in oriented noncrystalline PET fibers were investigated. The fibers exhibited two very distinct thermal responses depending on the fiber orientation. The local structure of the oriented noncrystalline PET chains as studied by the X-ray diffraction and FTIR spectroscopy revealed the mesophase structure with the well extended chain conformation in some fibers of high orientation. It was suggested that the oriented noncrystalline structure of PET consists of partially oriented noncrystalline phase and chain-extended noncrystalline phase. Our results demonstrated that the evolution of mesophase structure, i.e. chain-extended noncrystalline phase in the spin line not only led the drastic increase of packing density but also had a strong effect on thermal deformations upon post heat treatment. The amount of thermal shrinkage or the elongation reduced drastically in the fibers containing the mesophase. The high population of trans conformer and the strong inter-chain interactions of the extended chains provided the dimensional stability of the fibers during the thermal treatment.

Keywords: Thermal deformation; Oriented noncrystalline PET fiber; Mesophase structure

1. Introduction

Poly (ethylene terephthalate) (PET) is a commodity polymer found in numerous commercial applications in the form of fibers and films of different orientation and crystallinity. These applications are mainly originated from excellent processing properties of PET such as high glass transition temperature and slow crystallization rate, which enables one to control final morphologies. One of the primary processing modes of PET is the high-speed melt-spinning process. By controlling the spinning and quenching conditions, the polymer can take various degree of chain orientation and local packing density while maintaining the noncrystalline structures [1,2]. Depending on the morphological state the fibers exhibit various thermal properties upon post heat-treatment and further the physical and mechanical properties of final products. The post heat-treatment of as-spun PET fiber typically involves thermal deformations such as thermal shrinkage [2–11] or spontaneous elongation [11–16] at elevated temperatures near the transition temperature, whether the experiment is carried out under unconstraint or constraint sample condition, respectively. Such thermally induced deformations leading to dimensional changes upon post heat-treatment are irreversible and mainly dependent upon their initial chain orientations and crystallinities of the as-spun fibers [2]. It is well known that the thermal shrinkage of the as-spun fiber during post heat-treatment is ascribed to the recovery (disorientation) of oriented chains [6,8,9] and the spontaneous elongation is to the crystallization [12–14]. It can be then easily anticipated that those thermal deformations are highly dependent on the micro structures of the as-spun fibers such as crystallinity, orientation, and chain conformation.

During spinning process of PET, the polymer chains can be solidified into a noncrystalline structure by controlling the spinning speed, i.e. the degree of orientation. In general, the PET fibers at or below ~4800 m/min are still noncrystalline. The fibers spun above this take up velocity,

* Corresponding author. Tel.: +82 42 629 7504; fax: +82 42 626 8841
E-mail address: songhh@hannam.ac.kr (H.H. Song).

0032-3861/$ - see front matter © 2004 Elsevier Ltd. All rights reserved.
doi:10.1016/j.polymer.2004.12.004

on the other hand, begin to show crystalline order as revealed by the X-ray diffraction. One of the unique structural features to observe in the PET orientation is the mesophase structure found in some fibers of certain orientation. This mesophase is transient and disappears with the appearance of crystalline order either by the post thermal treatment or by the strain induced crystallization on further orientation. The existence of this metastable mesophase was initially studied decades ago by several workers [17–27]. Authors [28] were also able to observe this mesophase structure by uniaxially stretching the partially oriented noncrystalline PET fibers below the glass transition temperature. The mesophase was only found in those fibers stretched beyond the strain hardening region in S–S curve and the amount of mesophase increased with the orientation until it began to show the crystalline order. In a recent work by Kawakami et al. [29], the mesophase was also formed before the strain hardening when the amorphous PET is stretched above the glass transition temperature.

In this work, we focused our efforts to elucidate the effect of the microstructures of oriented chains, especially the existence of mesophase, on the thermal deformations. The local microstructures of the oriented PET fibers were carefully examined by the high resolution wide angle X-ray diffraction utilizing the synchrotron radiation and the FTIR spectroscopy, while the overall packing state was measured by the density measurement.

2. Experimental

2.1. Materials

High-speed melt-spun noncrystalline poly (ethylene terephthalate) (PET) fibers (named S1 ~ S6) were obtained from Hyosung Corporation. These six fibers were spun at different spinning speed (see Table 1 for the details), thus with different fiber orientation. The spinning temperature was 295 °C and the fiber was air quenched below the spinneret by blowing the quenching air (20 °C) at the speed of 0.4–0.5 m/s. The intrinsic viscosity of PET fiber was 0.64 dl/g which corresponds to 27,000 g/mol (M_n). The fibers in a bundle of ~1180 deniers were tested for all experiments.

2.2. Sample characterization

All characterizations on the fibers described below were performed before the heat treatment Wide angle X-ray diffraction (WAXD) experiments were performed utilizing a synchrotron X-ray source (2.5 GeV, 150 mA) at the 4C1 X-ray beamline in Pohang Accelerator Laboratory (PAL). The wavelength was 1.6083 Å and the collimated beam size was 0.3 mm × 0.3 mm. Two-dimensional WAXD patterns were collected using a position-sensitive area detector. Data collection time of each pattern was 23 s. The distance between sample and detector was calibrated with a benzoic acid (WAXD) standard. FTIR spectroscopy (Perkin Elmer, 1000PC) was used to scrutinize the conformational characteristics of each specimen. Unpolarized IR beam was used and the scan interval was 1 cm^{-1}. The fiber density was measured using a density gradient column filled with the *n*-heptane/CCl_4 mixture. Prior to the placement of samples into the density gradient column, samples were evaporated for 24 h at the room temperature.

2.3. Measurements of thermal deformation

To test the thermal shrinkage, the fiber bundles were transferred to a preheated oven (150 °C) and were kept for 30 min while maintaining the oven temperature constant. The fiber bundles were then removed from the oven and fiber length was measured after being cooled to the room temperature. The shrinkage reached a saturation value immediately after the heat treatment at 150 °C. For the thermal elongation, on the other hand, the fiber bundles were kept in the preheated oven (150 °C) for 2 h under the constrained condition to prevent the thermal shrinkage. The fiber length was measured after being removed from the oven. The spontaneous elongation of the fibers was a relatively slow process compared to the shrinkage process and the fiber length reached a equilibrium value in about 2 h at 150 °C.

Table 1
Sample characteristics and data from WAXD experiment

Sample name	Spinning speed (m/min)	Wide angle X-ray diffraction		
		F_{ON}	FWHM	d-spacing (Å)
S1	2500 (REG)	7.7	10.0	4.58
S2	5000 (HS)	12.1	9.5	4.53
S3	3200 (REG)	15.9	9.2	4.49
S4	4000 (REG)	23.1	8.8	4.47
S5	4300 (REG)	26.5	8.6	4.43
S6	4500 (REG)	28.4	8.5	4.36

(HS): additive modified as-spun fiber (high-speed as-spun fiber); (REG): regular as-spun fiber; F_{ON}: amorphous orientation parameter; FWHM and d-spacing for the amorphous halo.

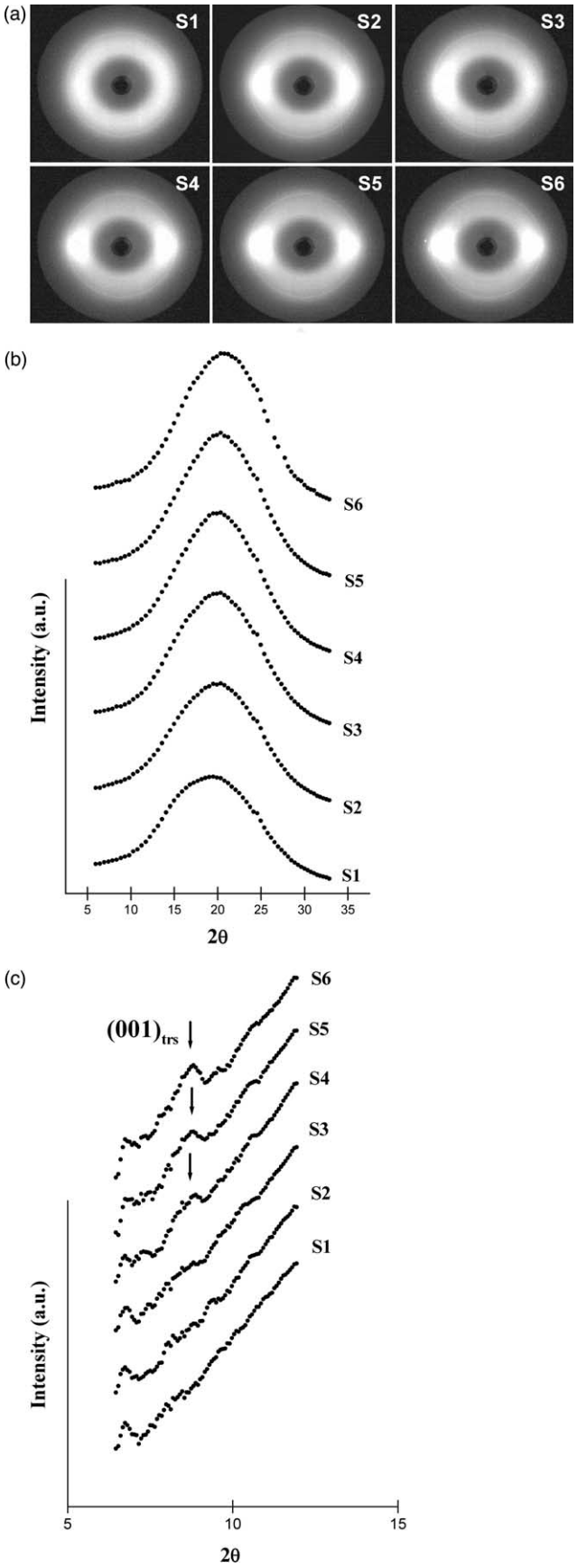

Fig. 1. (a) Two-dimensional wide angle X-ray difraction patterns of various high-speed melt-spun fibers; (b) equatorial and (c) meridional slices obtained from the pattern. Arrows in (c) indicate the reflection of the transient mesophase structure denoted as $(001)_{trs}$.

3. Results and discussion

3.1. Fine structure of oriented noncrystalline PET

The thermal responses of oriented noncrystalline fibsers upon post heat-treatment are highly dependent on the fine structural characteristics of fibers. We, therefore, begin with the structural characteristics of the fibers, before we discuss the thermal deformations of PET fibers such as thermal shrinkage and elongation.

The microstructural characteristics of as-spun PET fibers and resulting thermal responses during post heat-treatment are determined by the spinning conditions such as spinning temperature, take-up velocity and cooling condition. In a high-speed melt spinning process of PET fibers, strain-induced crystallization takes place when the take-up velocity reaches about 4800 m/min [1] and the crystallinity and crystal orientation increase with the take-up velocity. Below this critical take-up velocity, the oriented chains in the fiber are still noncrystalline. To investigate the relationship between the structure of as-spun fibers and their thermal responses such as shrinkage and spontaneous elongation upon heat-treatment, we focus our attention to the oriented amorphous fibers without any crystalline order. Two-dimensional wide angle X-ray diffraction patterns of PET fibers spun at different take-up velocities below 4800 m/min are plotted in Fig. 1(a). All patterns exhibit broad amorphous halo with orientation feature. Equatorial and meridional slices obtained from the two-dimensional WAXD patterns are also plotted in Fig. 1(b) and (c), respectively. As can be seen in the X-ray intensities all samples (S1–S6) show broad amorphous halo without any crystalline reflections in the equator, demonstrating the amorphous state of the oriented chains. Orientation parameter of the amorphous chains was then calculated from Eq. (1) [30].

$$F_{ON} = \frac{\int_0^{90} A_{ON}(\phi)\mathrm{d}\phi}{\int_0^{90}(A_{IA}(\phi) + A_{ON}(\phi))\mathrm{d}\phi} \times 10 \quad (1)$$

where, F_{ON} is the total oriented noncrystalline fraction or the amorphous orientation parameter. $A_{IA}(\phi)$ and $A_{ON}(\phi)$ are representing the relative diffraction areas of isotropic and oriented noncrystalline phase at any given azimuthal angle ϕ, respectively. Basic structural information associated with the oriented noncrystalline PET fibers such as amorphous orientation, full width at half maximum (FWHM) and d-spacing of amorphous halo are compared in Table 1. The amorphous orientation parameter (F_{ON}) of fiber increases with the take-up velocity. Decrease of FWHM and the shift of amorphous halo to a low d-spacing suggest the increase of local order with the fiber orientation.

In the meridional patterns (Fig. 1(c)), we do note a weak but discernible crystalline reflection, $(001)_{trs}$, whose spacing is ~10.4 Å. The peak is only observed in those fibers of S4, S5 and S6. But the peak is absent either when the chain orientation is not sufficient (S1, S2, S3) or when the orientation is high enough to result in strain-induced crystallization. The meridional peak is also found to be transient and disappears with the appearance of crystalline order upon elevating temperature. Observation of the transient meridional reflection in oriented PET films or fibers has been reported previously by a number of workers including authors [28]. In our recent report, we suggested that the two point meridional reflection arises from a layer-structure formed by ordering of chemical repeat units of PET across the oriented chains. Even though the chains within each layer are sufficiently extended, they are still noncrystalline and tilted against the fiber axis, resembling the smectic C-like mesophase.

In the current study, we also observe that the existence of this mesophase structure results in strong effects on some physical properties. In Fig. 2(a) and (b), density and integrated intensity of the meridional peak, i.e. amount of mesophase structure are plotted as a function of orientation parameter (F_{ON}) of each fiber. The results exhibit rapid increase in fiber density on and after sample S4. The drastic change in density can be attributed to the existence of mesophase structure of sample S4, S5 and S6. It is highly expected that well extended polymer chains in the mesophase promote much greater interactions between parallel chains. Song et al [28] has reported that the mesophase structure was found in those fibers stretched beyond the strain hardening region, demonstrating the nearly extended chains in the mesophase layer. Extended chain conformation (trans conformation in oxyethylene group) in mesophase can also be confirmed by the results of FTIR spectroscopy [5,31]. Fig. 3(a) and (b) describe the absorbance of two trans conformational state as a function amorphous orientation parameter (F_{ON}) of the fibers utilizing FT-IR spectroscopy. The characteristic absorption lines by trans conformer are at 845 and 972 cm^{-1} and by gauche conformer is at 898 cm^{-1}. The absorbance of trans conformer to that of gauche conformer derived from Eq. (2) can possibly give the quantity of trans conformer [5,31],

$$\text{Absorbance}(trans) = \frac{A_{trans}}{A_{gauche}} \tag{2}$$

where A_{trans} is the infra-red absorbance of the two trans absorption bands at 845 or 972 cm^{-1} and A_{gauche} is for the gauche isomer at 898 cm^{-1}. These characteristic absorption bands correspond to the 'wagging' of the oxy-ethylene group and to their trans and gauche conformations, respectively. The absorbance of trans conformer to that of gauche conformer as a function of F_{ON} plotted in Fig. 3(a) and (b) reveals nearly identical curve shape to those of density (Fig. 2(a)) and X-ray diffraction intensities of the mesophase structure (Fig. 2(b)). The drastic increase of trans conformer at the fiber S4, in which the mesophase begins to be observed, confirms the sudden increase of the well extended chains and thus much higher packing density.

3.2. Thermal deformations: shrinkage and elongation

The thermal responses of oriented noncrystalline fibers upon post heat-treatment are strongly influenced by structural characteristics of the chains such as internal chain conformation, orientation, and packing density. Thermal shrinkages of the fibers are plotted as a function of amorphous orientation parameter in Fig. 4. The thermal shrinkages are derived using Eq. (3) [11].

$$\text{Shrinkage}\ (\%) = \frac{L_0 - L}{L_0} \times 100 \tag{3}$$

where L_0 and L denote the initial and final length of fibers which were measured before and after elevating temperature to 150 °C, respectively. The fiber length was measured at the room temperature. The results illustrate two

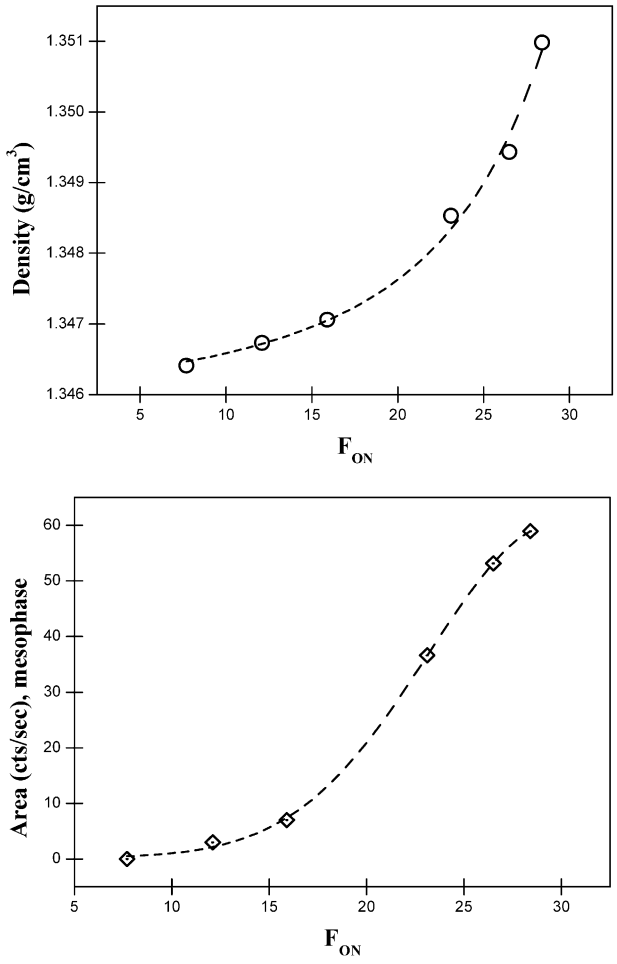

Fig. 2. Plot of (a) density and (b) integrated X-ray diffraction intensities from mesophase structure of each fiber as a function of orientation parameter (F_{ON}).

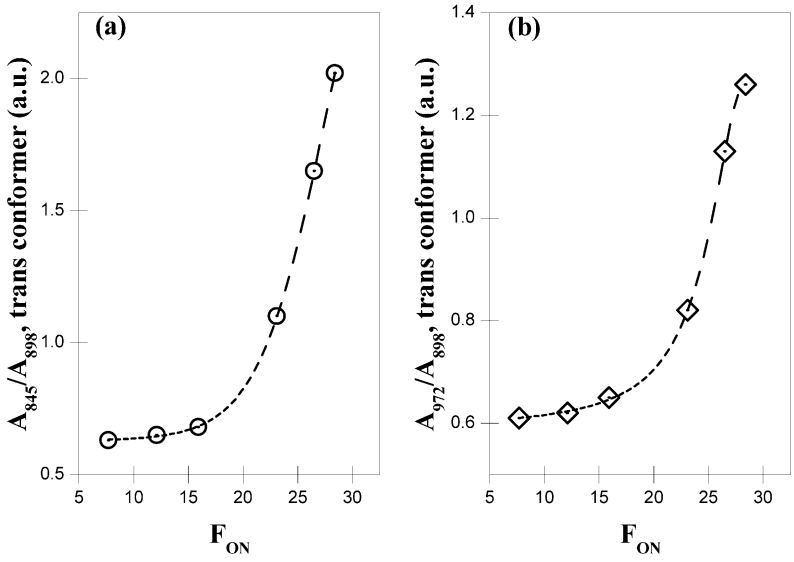

Fig. 3. Ratio of absorbances of trans conformer (845 and 972 cm^{-1}) to that of gauche conformer (898 cm^{-1}).

remarkably different responses on thermal shrinkage depending on the fiber orientation. Samples of relatively low F_{ON} (S1, S2, S3) show slight increase with the increase of F_{ON}. In contrast, fibers of higher F_{ON} (S4, S5, S6) show rapid decrease of the thermal shrinkage with the increase of F_{ON}. Furthermore, the thermal shrinkages of the fibers (S4, S5, S6) are far less than those of fibers (S1, S2, S3). It is quite unusual to note that the thermal shrinkage decreases with the chain orientation in fibers of relatively higher chain orientation. The thermal shrinkage originates from the randomization of the oriented chains and entropic recovery is the main driving force. The entropic gain, then, should be higher in those fibers of higher chain orientation. We recall that the three fibers (S4, S5, S6) show the meridional peak in X-ray diffraction patterns, indicating that the mesophase is formed and the amount of mesophase increases with the chain orientation. It is conceived that the chains in the mesophase are highly extended sufficient to yield the periodic order along the fiber axis even though there is no crystalline order. In randomizing process of the extended chains in the mesophase, these chains shall require somewhat high thermal energy to overcome the inter-chain interaction, which may surpass the entropic gain from the random recoiling process. On the other hand, in the fibers of low F_{ON} (S1, S2, S3) without containing the mesophase, the entropic gain would be greater than the thermal energy required for the chain recovery, allowing the higher thermal shrinkage.

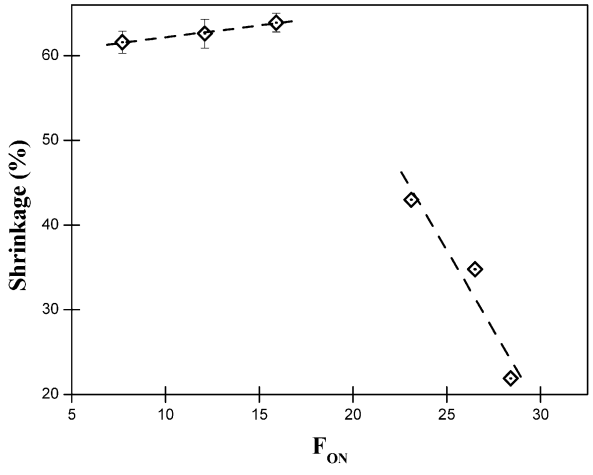

Fig. 4. Thermal shrinkage of fibers vs. F_{ON}.

Another dimensional change in the fiber length observed during the thermal treatment of the oriented noncrystalline PET is the spontaneous thermal elongation. When the fibers are heat-treated under the constraint condition (length held constant) to prevent the initial thermal shrinkage, irreversible spontaneous elongation is accompanied with the micro structural changes. Because this thermal elongation originates from the conformation change from gauche to trans via crystallization, it strongly depends upon the initial microstructure of the chains in the as-spun fibers. Spontaneous elongations measured at 150 °C under the constraint condition for the six fibers are compared in Fig. 5. Spontaneous elongation was measured by the following equation [11],

$$\text{Elongation } (\%) = \frac{L - L_0}{L_0} \times 100 \tag{4}$$

where L_0 and L denote the initial and the final fiber length, respectively. The results also exhibit two distinct behaviors in thermal elongation depending on the fiber orientation. For the fibers (S1, S2, S3) of low F_{ON}, the amount of elongation is large and decreases rapidly with the increase of fiber orientation. On the contrary, in the fibers (S4, S5, S6) of high orientation, very little dimensional change is noted. As discussed previously, the thermal elongation is due to the

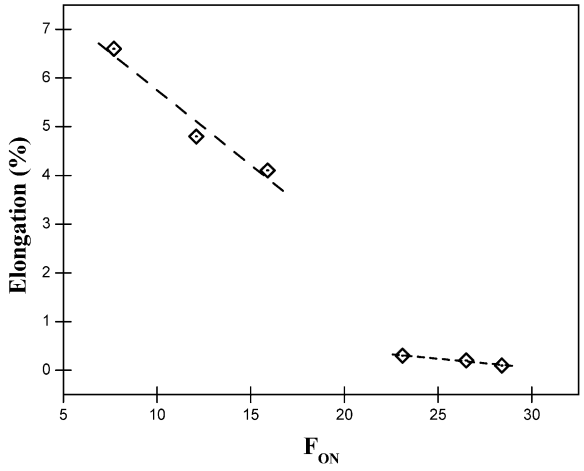

Fig. 5. Thermal elongation of fibers vs. F_{ON}.

gauche to trans conformation change associated with the crystallization. The amount of thermal elongation is closely related to the initial fraction of trans conformer, therefore, the overall orientation state in the sample. In the fibers of relatively low chain orientation (S1, S2, S3), the population of gauche conformer is relatively high and shall decrease rapidly with the fiber orientation. In those fibers (S4, S5, S6) of high orientation, on the other hand, the prevailing extended chains of trans conformer, as evidenced by the existence of mesophase, result in a very little gain in fiber length after the crystallization.

In general the microstructure of oriented amorphous fiber can be ideally separated into isotropic amorphous and oriented noncrystalline phase [30]. In an oriented noncrystalline phase, however, we note outstanding differences in microstructures and many physical properties including the thermal deformations depending on the overall fiber orientation. Our results suggest that there is a critical stage in the chain orientation where the chains promote an extended conformation and begin to exhibit mesophase-like characteristics. Now we propose that the oriented noncrystalline phase consists of two phases, i.e. partially oriented noncrystalline phase and chain-extended noncrystalline phase. Fig. 6 represents the schematic illustration of the suggested oriented noncrystalline phases (partially oriented and chain-extended) and their thermal responses to the heat treatment. The structures of oriented chains in fibers of low F_{ON} (S1, S2, S3) can be described by the partially oriented noncrystalline phase and those of high F_{ON} (S4, S5, S6) are mainly by the chain-extended noncrystalline phase. In the chain-extended noncrystalline phase, the bundles of extended chains and corresponding packing state of mesophase are emphasized. As discussed previously, the dimensional stability against the thermal treatment observed in the fibers (S4, S5, S6) are also depicted in the figure. The increased packing density in the extended chain bundles requires high thermal energy in recoiling process which apparently dominates the entropy gain through the randomizing process.

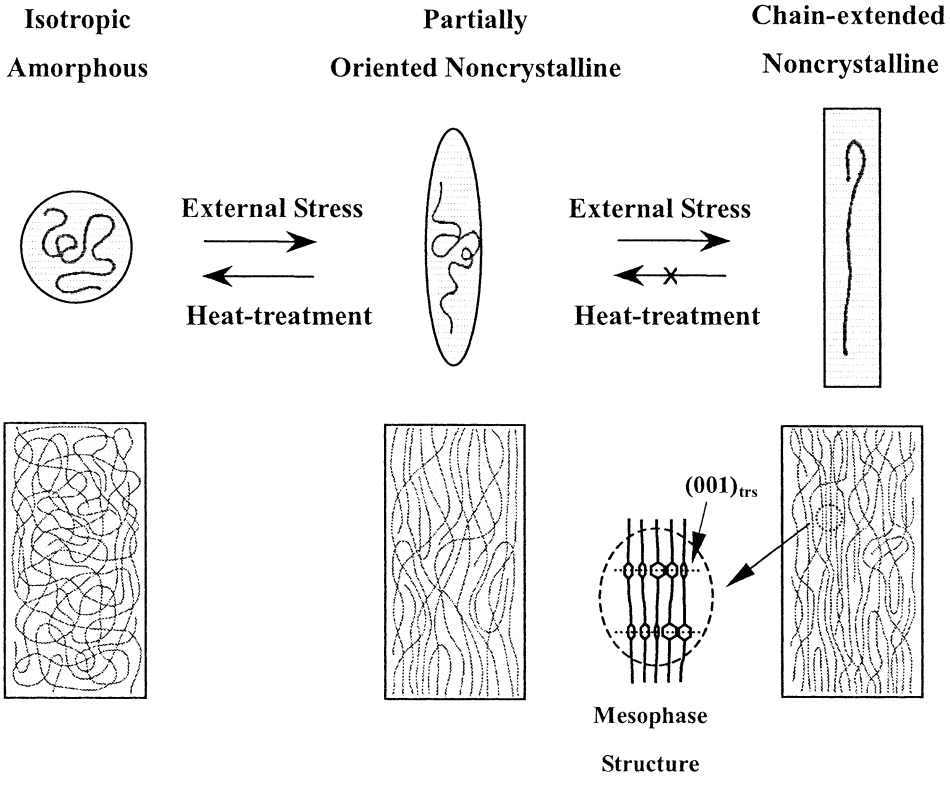

Fig. 6. Schematic illustrations of partially oriented and extended chains and their thermal responses to the heat-treatment.

4. Conclusions

It was suggested that the oriented noncrystalline PET chains consist of partially oriented noncrystalline phase and chain-extended noncrystalline phase. The advent of the extended noncrystalline phase requires certain degree of chain orientation, but which is not high enough to yield strain induced crystallization. The drastic change of packing density with the increase of F_{ON} in oriented noncrystalline PET fiber was observed and the results were closely related to the promotion of chain-extended phase and the mesophase structure in the fibers. Thermal deformations such as thermal shrinkage or elongation were also drastically reduced in the fibers containing the mesophase, i.e. the chain-extended noncrystalline phase. In randomizing process of the extended chains in the mesophase, the chains shall require high thermal energy to overcome the inter-chain interaction, which is greater than the entropic gain from the random coiling process, thus resulting in the drastic reduction in the thermal shrinkage. The reduction of the thermal elongation, originating from the *gauche*-to-*trans* conformation change, can also be attributed to the high population of trans conformer in the chain-extended noncrystalline phase.

Acknowledgements

This work was financially supported by the Hannam University Research Fund (2003). The X-ray diffraction experiment was performed at the 4C1 beam line in Pohang Accelerator Laboratory.

References

[1] Ziabicki A, Kawai H, editors. High-speed fiber spinning. New York: Intersciences; 1985.
[2] Grebowicz JS, Brown H, Chuah H, Olvera JM, Wasiak A, Sajkiewicz A, Ziabicki A. Polymer 2001;42:7153.
[3] Shimizu J, Okui N, Kaneko A, Toriumi K. Sen-I Gakkaishi 1978;34: T64.
[4] Heuvel HM, Huisman R. J Appl Polym Sci 1978;22:2229.
[5] Wu G, Yoshida T, Cuculo JA. Polymer 1998;39:6473.
[6] Wilson MPW. Polymer 1974;15:277.
[7] Statton WO, Koenig JL, Hannon MJ. J Appl Polym Sci 1965;9:2661.
[8] Prevorsek DC, Tirpak GA, Harget PJ, Reimschuessel AC. J Macromol Sci Phys 1974;B9:733.
[9] Nobbs JH, Bower DI, Ward IM. Polymer 1976;17:25.
[10] Oswald HJ, Turi EA, Harget PJ, Khanna YP. J Macromol Sci Phys 1977;B13:231.
[11] Pereira JRC, Porter RS. Polymer 1984;25:877.
[12] Smith WH, Saylor CP. J Res Natl Bur Stand 1938;21:257.
[13] Alfrey T, Mark H. J Phys Chem 1942;46:112.
[14] Bosley DE. J Polym Sci C 1967;20:77.
[15] Mandelkern L, Roberts DE, Diorio AF, Posner AS. J Am Chem Soc 1959;81:4148.
[16] Pinnock PR, Ward IM. Trans Faraday Soc 1966;62:1308.
[17] Bonart R. Kolloid-Z 1966;213:1.
[18] Bonart R. Kolloid-Z 1966;213:16.
[19] Bonart R. Kolloid-Z 1968;231:438.
[20] Asano T, Seto T. Polym J 1973;5:72.
[21] Asano T, Baltá Calleja FJ, Flores A, Tanikaki M, Mina MF, Sawatari C, Itagaki H, Takahashi H, Hatta I. Polym J 1999;40:6475.
[22] Yeh GSY, Geil PH. J Macromol Sci B 1967;1:235.
[23] Yeh GSY, Geil PH. J Macromol Sci B 1967;1:251.
[24] Gorlier E, Haudin JM, Billon N. Polymer 2001;42:9541.
[25] Mahendrasingam A, Martin C, Fuller W, Blundell DJ, Oldman RJ, Harvie JL, Mackerron DH, Riekel C, Engstrom P. Polymer 1999;40: 5553.
[26] Mahendrasingam A, Martin C, Fuller W, Blundell DJ, Oldman RJ, Mackerron DH, Harvie JL, Riekel C. Polymer 2000;41:1217.
[27] Welsh L, Blundell DJ, Windle AH. Macromolecules 1998;31:7562.
[28] Keum JK, Kim JM, Lee SM, Song HH, Son Y, Choi J, Im SS. Macromolecules 2003;36:9873.
[29] Kawakami D, Hsiao B, Ran S, Burger C, Fu B, Sics I, Chu B, Kikutani T. Polymer 2004;45:905.
[30] Wu G, Jiang J, Tucker PA, Cuculo JA. J Polym Sci, Part B: Polym Phys 1996;34:2035.
[31] Wu G, Yoshida T, Cuculo JA. Polymer 1997;38:109131. Wu G, Yoshida T, Cuculo JA. Polymer 1997;38:1091.